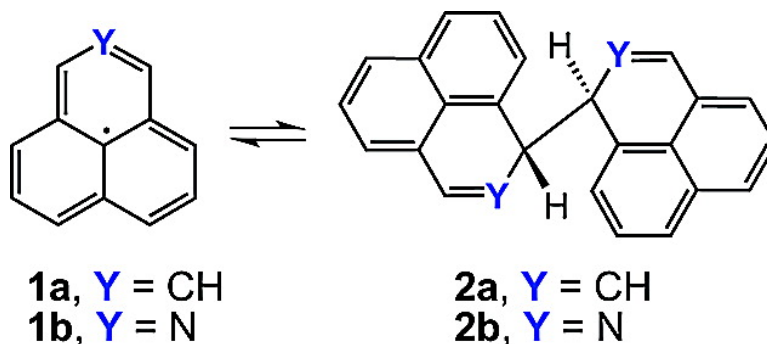


## Synthesis, Characterization, and Coordination Chemistry of the 2-Azaphenalenyl Radical

Shijun Zheng, Jie Lan, Saeed I. Khan, and Yves Rubin

*J. Am. Chem. Soc.*, **2003**, 125 (19), 5786-5791 • DOI: 10.1021/ja029236o • Publication Date (Web): 19 April 2003

Downloaded from <http://pubs.acs.org> on March 26, 2009



### More About This Article

Additional resources and features associated with this article are available within the HTML version:

- Supporting Information
- Links to the 10 articles that cite this article, as of the time of this article download
- Access to high resolution figures
- Links to articles and content related to this article
- Copyright permission to reproduce figures and/or text from this article

[View the Full Text HTML](#)



## Synthesis, Characterization, and Coordination Chemistry of the 2-Azaphenalenyl Radical

Shijun Zheng, Jie Lan, Saeed I. Khan, and Yves Rubin\*

Contribution from the Department of Chemistry and Biochemistry, University of California, Los Angeles, California 90095-1569

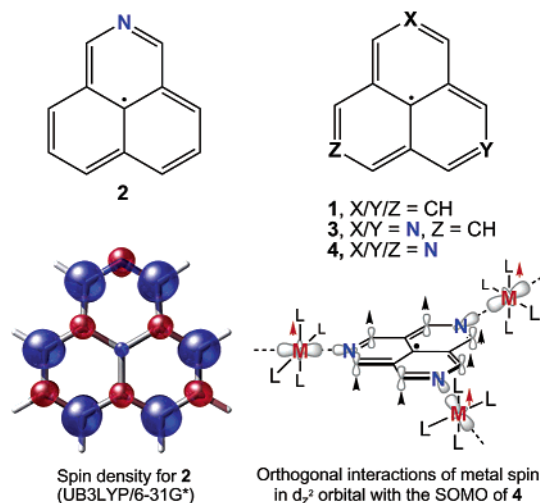
Received November 6, 2002; E-mail: rubin@chem.ucla.edu

**Abstract:** The 2-azaphenalenyl radical **2** has been synthesized and characterized by ESR spectroscopy. Variable-temperature ESR measurements were carried out on both the phenalenyl (**1**) and the 2-azaphenalenyl (**2**) radicals. The phenalenyl radical **1** has the known propensity to dimerize at temperatures below 20 °C, but unexpectedly less so than originally reported. The first experimental measurement of bond dissociation enthalpy for the dimerization of the phenalenyl radical **1** was obtained in CCl<sub>4</sub> (11.34 ± 0.11 kcal/mol) and toluene (9.8 ± 0.7 kcal/mol). The 2-azaphenalenyl radical **2** does not show a propensity to dimerize over the measurable temperature range (220–330 K), but does so in the presence of Cu(hfac)<sub>2</sub> (hfac = hexafluoroacetylacetonate). The latter complex was characterized by X-ray crystallography.

### Introduction

The phenalenyl system forms a relatively stable organic  $\pi$ -radical (**1**) having  $D_{3h}$  symmetry, along with a stable cation and anion because of its particular orbital configuration (Chart 1).<sup>1</sup> With these features, radical **1** and its derivatives have been investigated as components of conducting materials and organic ferromagnets.<sup>2</sup> In the context of molecule-based magnets,<sup>3,4</sup> the dimension, geometry, and arrangement of molecules in a solid are important factors determining spin order, because magnetic interactions are strongly dependent on orbital exchange terms and spin separation. One of the most successful strategies in this field has relied on strong, mediating antiferromagnetic exchange interactions in metal–organic radical complexes that give ferrimagnetic states with  $T_c$ 's up to 400 K.<sup>5</sup> With this approach, a key interaction dictates the alignment of remaining spins in an oligomeric complex. This primary interaction is often complicated by weaker interchain interactions that counter intrachain spin ordering; thus, higher order two- and three-dimensional networks are necessary to promote efficient spin ordering, a design parameter that has been pursued more recently.<sup>5,6</sup> Ultimately, molecule-based ferromagnet strategies should benefit from the advantages of geometric and electronic

Chart 1



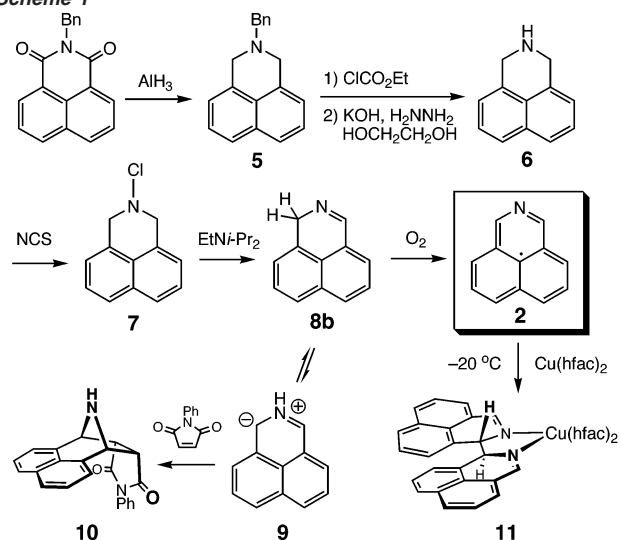
tunability of organic systems, which could open new vistas in specific applications, for example, nonvolatile memory.<sup>6</sup>

We are exploring strategies to promote ferromagnetic ordering in two- or three-dimensional organic radical–transition metal complexes, one of them using the 2,5-di- and 2,5,8-triaza-

- (1) (a) Reid, D. H. *Tetrahedron* **1958**, *3*, 339–352. (b) Sogo, P. B.; Nakazaki, M.; Calvin, M. *J. Chem. Phys.* **1957**, *26*, 1343–1345. (c) Gerson, F. *Helv. Chim. Acta* **1966**, *49*, 1463–1467.  
(2) (a) Koutentis, P. A.; Chen, Y.; Cao, Y.; Best, T. P.; Itkis, M. M.; Beer, L.; Oakley, R. T.; Cordes, A. W.; Brock, C. P.; Haddon, R. C. *J. Am. Chem. Soc.* **2001**, *123*, 3864–3871 and references therein. (b) Goto, K.; Kubo, T.; Yamamoto, K.; Nakasuji, K.; Sato, K.; Shiomi, D.; Takui, T.; Kubota, M.; Kobayashi, T.; Yakusi, K.; Ouyang, J. *J. Am. Chem. Soc.* **1999**, *121*, 1619–1620. (c) Morita, Y.; Aoki, T.; Fukui, K.; Nakazawa, S.; Tamaki, K.; Suzuki, S.; Fuyuhiko, A.; Yamamoto, K.; Sato, K.; Shiomi, D.; Naito, A.; Takui, T.; Nakasuji, K. *Angew. Chem., Int. Ed.* **2002**, *41*, 1793–1796.  
(3) (a) Miller, J. S.; Epstein, A. J.; Reiff, W. M. *Chem. Rev.* **1988**, *88*, 201–220. (b) Kahn, O. *Molecular Magnetism*; VCH: New York, **1993**. (c) Miller, J. S.; Epstein, A. J. *Angew. Chem., Int. Ed. Engl.* **1994**, *33*, 385–415.  
(4) (a) Iwamura, H. *Pure Appl. Chem.* **1993**, *65*, 57–64. (b) Rajca, A. *Chem. Rev.* **1994**, *94*, 871–893.

- (5) (a) Kahn, O.; Pei, Y.; Verdager, M.; Renard, J. P.; Sletten, J. *J. Am. Chem. Soc.* **1988**, *110*, 782–789. (b) Gadet, V.; Mallah, T.; Castro, I.; Verdager, M.; Veillet, P. *J. Am. Chem. Soc.* **1992**, *114*, 9213–9214. (c) Ezuhara, T.; Endo, K.; Matsuda, K.; Aoyama, Y. *New J. Chem.* **2000**, *24*, 609–613. (d) Caneschi, A. G. D.; Sessoli, R.; Rey, P. *Acc. Chem. Res.* **1989**, *22*, 392–398. (e) Manriquez, J. M.; Yee, G. T.; McLean, S. R.; Epstein, A. J.; Miller, J. S. *Science* **1991**, *252*, 1415–1417. (f) Barclay, T. M.; Hicks, R. G.; Lemaire, M. T.; Thompson, L. *Chem. Commun.* **2000**, 2141–2142. (g) Karasawa, S.; Kumada, H.; Koga, N.; Iwamura, H. *J. Am. Chem. Soc.* **2001**, *123*, 9685–9686. (h) Fujita, W.; Awaga, K. *J. Am. Chem. Soc.* **2001**, *123*, 3601–3602. (i) Lau, V. C.; Berben, L. A.; Long, J. R. *J. Am. Chem. Soc.* **2002**, *124*, 9042–9043.  
(6) (a) Sato, O.; Iyoda, T.; Fujishima, A.; Hashimoto, K. *Science* **1996**, *271*, 49–50. (b) Verdager, M. *Science* **1996**, *272*, 698–699. (c) Guillaume Rombaut, G.; Verelst, M.; Golhen, S.; Ouahab, L.; Mathonière, C.; Kahn, O. *Inorg. Chem.* **2001**, *40*, 1151–1159.

## Scheme 1



phenalenyl radicals (**3**, **4**) as spin couplers. DFT calculations (UB3LYP/6-31G\*) show that the  $\beta$ -spin densities for the series of the 2-aza-, 2,5-diaza-, and 2,5,8-triazaphenalenyl radicals (**2**–**4**) reside mainly at the 1,3,4,6,7,9-positions, in a configuration similar to that of the parent phenalenyl radical **1**, as one would expect (Chart 1, Figure 2).<sup>1b</sup> Coordination of appropriate transition metals (e.g., Ni(II), Cu(II)) to the radical ligands **3** and **4** may induce significant ferromagnetic exchange interactions due to either (or both) spin polarization interactions<sup>7</sup> or the interaction arising from the orthogonal relationship of singly occupied  $d_{z^2}$  and/or  $d_{x^2-y^2}$  orbitals on such transition metals with the spin  $\pi$ -orbitals of the radicals **3** and **4** (Chart 1).<sup>5f–h</sup>

Even though the phenalenyl radical **1** was discovered already a half a century ago, the 2,5,8-tri-*tert*-butyl-1,3-diazaphenalenyl radical is the only reported azaphenalenyl radical.<sup>2c</sup> However, the 2,5,8-triazaphenalenyl radical **4** or any of its derivatives would be better suited for three-dimensional assemblies with its higher coordination number and lesser steric hindrance.<sup>8</sup> Here we report the synthesis and characterization of the parent 2-azaphenalenyl radical **2** as a model system to study the effect of N-substitution on the phenalenyl system.

## Results and Discussion

**Synthesis.** Radical **2** was synthesized in six steps from *N*-benzylphthalimide (Scheme 1). Reduction by  $\text{AlH}_3$  gave the tertiary amine **5** in 89% yield. Debenzylation of **5** by acylation with ethyl chloroformate and  $\text{KOH}/\text{NH}_2\text{NH}_2$  treatment afforded the secondary amine **6** in 89% yield, which was quantitatively converted to the *N*-chloramine **7** with *N*-chlorosuccinimide. The dehydrochlorination of **7** with a mild base (e.g., diisopropylethylamine, triethylamine) affords the unstable 2-azaphenalenyl radical **8b**, characterized by in situ  $^1\text{H}$  NMR and EI mass spectroscopy. Compound **8b** easily isomerizes to the reactive azomethine ylide **9** in the presence of excess base, the latter characterized by trapping with *N*-phenylmaleimide as found in a different study.<sup>9</sup> Compound **8b** is very easily oxidized by air

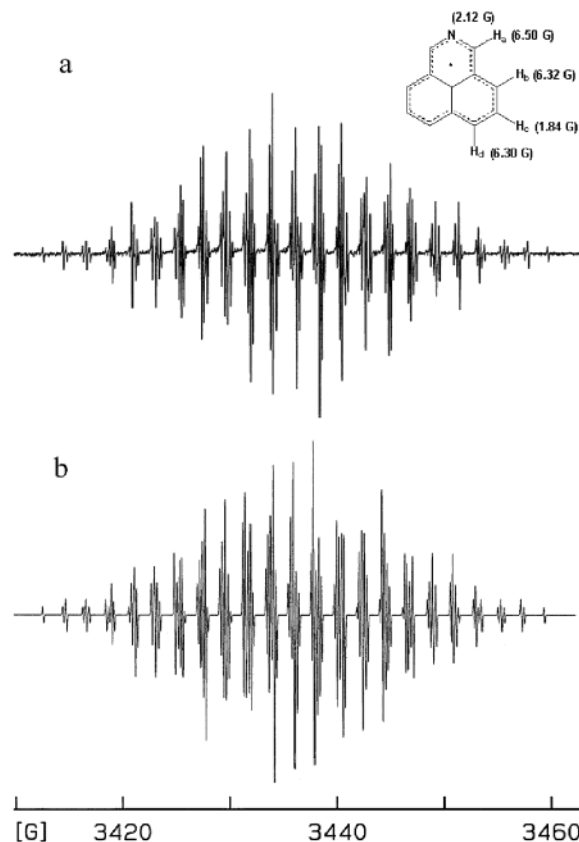


**Figure 1.** (a) ESR spectrum of radical **2** in toluene at 25 °C. (b) Simulated ESR spectrum of radical **2** (WinEPR).

**Table 1.** Experimental and Calculated HFCCs for Radical **2**

	experimental <sup>a</sup> (Gauss)	EPR-III (Gauss)	EPR-II (Gauss)
$a_{\text{Ha}}$	6.50	−7.18	−7.28
$a_{\text{Hb}}$	6.32	−6.87	−7.00
$a_{\text{Hc}}$	2.12	2.52	2.61
$a_{\text{Hd}}$	6.30	−6.85	−6.98
$a_{\text{N}}$	1.84	−2.04	−2.15

<sup>a</sup> Experimental values are absolute.

to the yellow-green radical **2**, which decomposes much more slowly in the presence of excess air to give several polar products and baseline material. Attempts at isolation by column chromatography ( $\text{SiO}_2$ , Florisil) led to complete decomposition even though a streaking yellow-green spot is observable by TLC ( $R_f = 0.3$ ,  $\text{CH}_2\text{Cl}_2$ ). However, a sealed ESR tube containing compound **8b** in toluene prepared from  $\sim 1.0$  mg ( $\sim 0.01$  mmol) of chloramine **7** (after filtration of the ammonium salts) and a limited amount of air ( $\sim 1$  mL,  $\sim 0.01$  mmol) generates radical **2** over 2 days, giving the strong ESR signal shown in Figure 1. Without excess air, radical **2** is stable in solution in a sealed tube for months.

**Calculations.** Unrestricted density functional calculations with the B3LYP model have been tested and validated in a number of studies on organic radicals.<sup>10</sup> Optimized geometries in the gas phase and harmonic vibrational frequencies of the phenalenyl (**1**,  $D_{3h}$ ), 2-azaphenalenyl (**2**,  $C_{2v}$ ), 2,5-diazaphenalenyl (**3**,  $C_{2v}$ ), and 2,5,8-triazaphenalenyl (**4**,  $D_{3h}$ ) radicals were obtained at the UB3LYP/6-31G\* level of theory using the

(7) (a) Oshio, H. *J. Chem. Soc., Chem. Commun.* **1991**, 240–241. (b) Mitsubori, S.; Ishida, T.; Nogami, T.; Iwamura, H. *Chem. Lett.* **1994**, 285–288. (c) McCleverty, J. A.; Ward, M. D. *Acc. Chem. Res.* **1998**, *31*, 842–851.  
 (8) For the recent synthesis of the perchloro-2,5,8-triazaphenalenyl radical, see: Zheng, S.; Thompson, J. D.; Toncheva, A.; Khan, S. I.; Rubin, Y. *J. Am. Chem. Soc.*, submitted.  
 (9) Sha, C.; Wang, D. *Tetrahedron* **1994**, *50*, 7495–7502.

(10) Boesch, S. E.; Wheeler, R. A. *J. Phys. Chem. A* **1997**, *101*, 5799–5804.

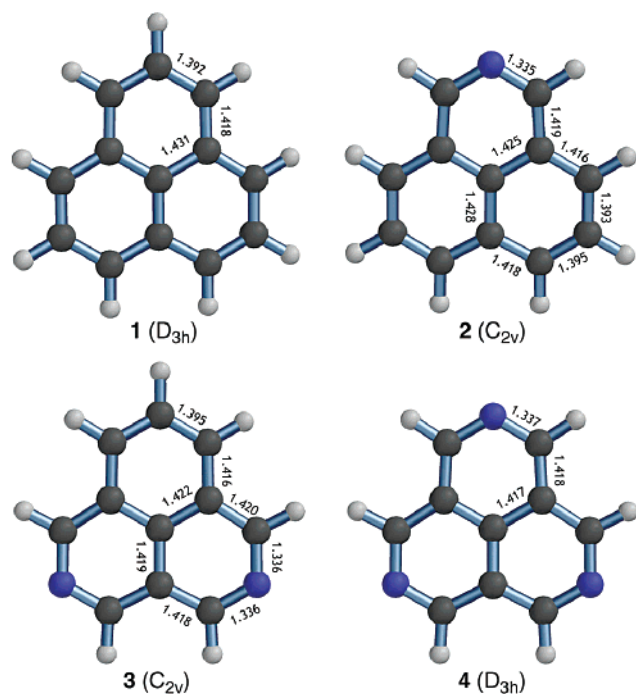


**Figure 2.** Calculated structures (UB3LYP/6-31G\*) and selected bond lengths for the phenalenyl (1), 2-azaphenalenyl (2), 2,5-diazaphenalenyl (3), and 2,5,8-triazaphenalenyl (4) radicals.

**Table 2.** Frontier Orbital Energies (eV) of the Radicals 1–4 (UB3LYP/6-31G\*)

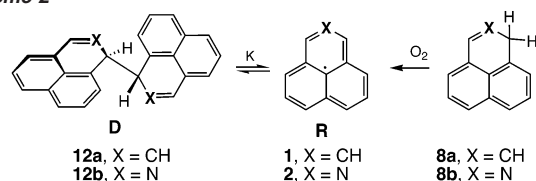
radical	HOMO ( $\alpha$ )	SOMO ( $\beta$ )	LUMO ( $\alpha$ )
phenalenyl (1)	−4.384	−2.447	−0.204
2-azaphenalenyl (2)	−4.681	−2.727	−0.767
2,5-diazaphenalenyl (3)	−4.986	−3.014	−1.054
2,5,8-triazaphenalenyl (4)	−5.298	−3.308	−1.345

Gaussian 98 package (Figure 2).<sup>11</sup> To assist with assignments, ESR hyperfine coupling constants (hfcc) of the 2-azaphenalenyl radical **2** were calculated on the basis of the optimized structure using both EPR-II and EPR-III basis sets within Gaussian 98 (Table 1).<sup>12</sup>

The bond distances (Å) are all within normal aromatic lengths, the shorter C–N bond corresponding to that of a six-membered ring nitrogen heterocycle (Figure 2). These bond lengths indicate complete delocalization, and the molecules are flat, as would be expected.

Table 1 contains both experimental and calculated ESR isotropic hyperfine coupling constants. Results from both EPR-II and EPR-III basis sets are reported. These values are in agreement but consistently higher than the experimental values, with EPR-III numbers that are slightly more accurate. Because

**Scheme 2**



these are gas-phase values, solvent effects are not included and probably account for the overestimation of the H and N coupling constants.<sup>13</sup>

The frontier orbital energies of the phenalenyl, 2-azaphenalenyl, 2,5-diaza-, and 2,5,8-triazaphenalenyl radicals 1–4 are reported in Table 2. The HOMO, SOMO, and LUMO energies decrease steadily as the substitution of a CH group by a nitrogen atom in these systems increases, as would be expected. As a consequence, a reduction in the reactivity of radicals 1–4 can be expected with higher nitrogen substitution, as can be seen from the dimerization experiments reported below for the phenalenyl radical **1** and 2-azaphenalenyl radical **2**.

**ESR Spectroscopy.** The ESR spectrum of radical **2**, with an observed  $g$  value of 2.0031 indicating that it is a carbon-based free radical, shows a well-resolved set of 112 nonoverlapping lines out of the 135 theoretical lines for H and N splittings (Figure 1). The hyperfine coupling constants (hfcc's) were obtained by line shape analysis (Table 1). The hfcc values show that the substitution of a nitrogen atom at the 2-position of the phenalenyl radical does not change the spin distribution significantly as shown by the calculations (Chart 1). However, there is slightly higher  $\beta$ -spin density at the 1,3-positions directly next to the nitrogen atom, due to the larger C–N bond order, than at the remaining 4,6,7,9-positions.

**Variable-Temperature ESR Experiments.** The dimerization of the phenalenyl radical **1** to the  $\sigma$ -bonded 2,2'-biphenylene **12a** (Scheme 2) was reported by Gerson in 1966.<sup>1c</sup> The reported ESR signal loss at  $-25$  °C in  $\text{CCl}_4$  occurs near the melting point of this solvent. However, our observations find that more subtle effects are taking place: the tendency of phenalenyl radical **1** to dimerize at lower temperatures is clearly confirmed (Figures 3 and 4),<sup>1c,9</sup> but there is an incomplete signal loss at  $-65$  °C when the solvent is changed from  $\text{CCl}_4$  (Figure 4) to toluene (Figure 3).<sup>14</sup> In addition, the ESR signal intensity in Gerson's experiments showed a steady exponential increase in  $\text{CCl}_4$  from 10 to 60 °C that is not corroborated by our experiments, but which may perhaps be explained by an accelerated formation of radical through oxidation if excess air was present (see below).<sup>1c</sup>

The phenalenyl radical **1** was generated by air oxidation of phenalene **8a** ( $\sim 0.01$  mM in  $\text{CCl}_4$  or toluene).<sup>1</sup> The toluene solution was left standing for 2 months in a sealed quartz tube prior to measurement to consume all of the available air. Several heating and cooling cycles were performed for each experiment, confirming the reversibility of the dimerization. A steady decrease but incomplete loss of signal intensity occurs down to  $-65$  °C (Figure 3),<sup>14</sup> while an asymptotic limit is reached above 25 °C. Interestingly, when the radical was formed in  $\text{CCl}_4$  by standing for 24 h at room temperature, as in Gerson's

(11) Frisch, M. J.; Trucks, G. W.; Schlegel, H. B.; Scuseria, G. E.; Robb, M. A.; Cheeseman, J. R.; Zakrzewski, V. G.; Montgomery, J. A., Jr.; Stratmann, R. E.; Burant, J. C.; Dapprich, S.; Millam, J. M.; Daniels, A. D.; Kudin, K. N.; Strain, M. C.; Farkas, O.; Tomasi, J.; Barone, V.; Cossi, M.; Cammi, R.; Mennucci, B.; Pomelli, C.; Adamo, C.; Clifford, S.; Ochterski, J.; Petersson, G. A.; Ayala, P. Y.; Cui, Q.; Morokuma, K.; Malick, D. K.; Rabuck, A. D.; Raghavachari, K.; Foresman, J. B.; Cioslowski, J.; Ortiz, J. V.; Stefanov, B. B.; Liu, G.; Liashenko, A.; Piskorz, P.; Komaromi, I.; Gomperts, R.; Martin, R. L.; Fox, D. J.; Keith, T.; Al-Laham, M. A.; Peng, C. Y.; Nanayakkara, A.; Gonzalez, C.; Challacombe, M.; Gill, P. M. W.; Johnson, B. G.; Chen, W.; Wong, M. W.; Andres, J. L.; Head-Gordon, M.; Replogle, E. S.; Pople, J. A. *Gaussian 98*, revision A.9; Gaussian, Inc.: Pittsburgh, PA, 1998.

(12) Barone, V. In *Recent Advances in Density Functional Theory*, Part 1; Cong, D. P., Ed.; World Scientific Publishing Co.: Singapore, 1995; p 287.

(13) Cirujeda, J.; Vidal-Gancedo, J.; Jergens, O.; Mota, F.; Novoa, J.; Rovira, C.; Veciana, J. *J. Am. Chem. Soc.* **2000**, *122*, 11393–11405.

(14) The signal noise levels below  $-65$  °C made a quantitative measurement of the intensity data unreliable; thus, the lower limit of signal intensity could not be extrapolated.

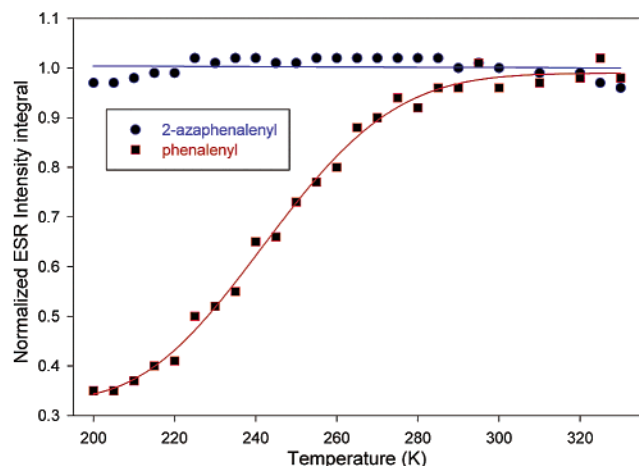


**Figure 3.** Plots of integrated ESR signal intensities (normalized) versus temperature for the phenalenyl (**1**,  $\sim 10^{-7}$  M) and 2-azaphenalenyl (**2**,  $\sim 0.5 \times 10^{-7}$  M) radicals in toluene.

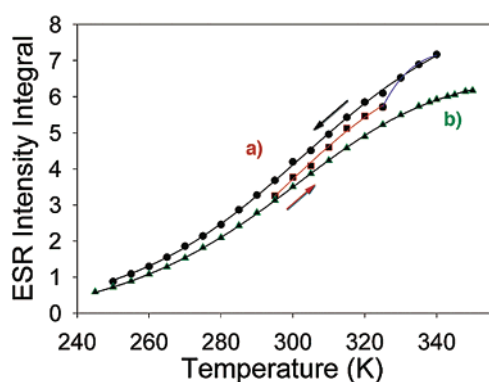


**Figure 4.** VT experiments with the phenalenyl radical **1** in  $\text{CCl}_4$  ( $\sim 10^{-6}$  M) using conditions similar to those in ref 1c: (a) After the solution was stored at 25 °C for 24 h in a quartz tube sealed under air, ESR intensity data were obtained by heating from 295 to 340 K, followed by cooling to 250 K. (b) After the same sample was “aged” for 48 h at 65 °C as described in the text; ESR intensity data are for both heating and cooling cycles. Curve fits were obtained for the data points shown in the different colors.

experiments,<sup>1c</sup> we observed a peculiar behavior of the ESR intensity curve if the heating cycle was carried out prior to cooling (Figure 4a). There was a sudden pickup in the concentration of radical **1** at 325 K (52 °C, blue colored curve fit), but this behavior vanished after keeping the sample sealed *under air* for longer periods of time ( $\sim 2$  months at 25 °C or by “aging” the sample for 48 h at 65 °C with gentle swirling of the solution-containing ESR tube using a Kugelrohr apparatus; Figure 4b). We attribute this effect to an accelerated formation of the phenalenyl radical **1** above 50 °C through air oxidation of phenalene **8a**. The longer storage period or “aging” process depletes all of the available  $\text{O}_2$ , the VT experiments giving then a proper asymptotic limit to the intensity increase (Figure 4b).

The bond dissociation enthalpy of the phenalenyl radical dimer **8a** was determined from the ESR signal intensity versus temperature data. At the asymptotic limit, it can be assumed that all of the dimer **12a** (D) is dissociated into the radical **1** (R) to give a radical concentration  $[\text{R}]_{\text{max}} = 2C_0$  ( $C_0$  is the original dimer concentration before dissociation) because the decomposition of radical **1** under these conditions is negligible (relative ESR signal intensities remained constant throughout several heating/cooling cycles). The value of  $[\text{R}]_{\text{max}}$  was determined by calibration with a solution of 3-oxo-TEMPO of

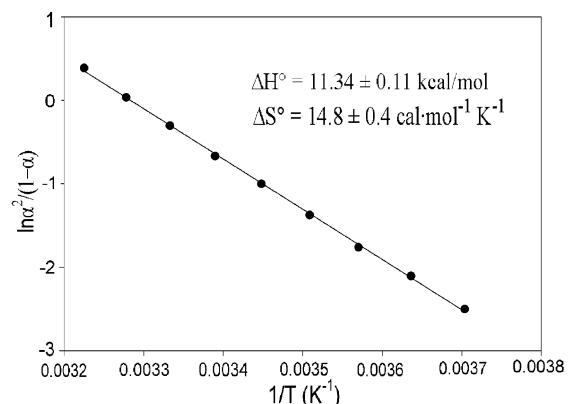


**Figure 5.** Plot of  $\ln \alpha^2/(1 - \alpha)$  versus  $1/T$  for radical **1** between 270 and 310 K in  $\text{CCl}_4$ .

known concentration.<sup>15</sup> As a result, ignoring the temperature effect on the ESR intensity, which is negligible,<sup>16</sup> the dissociation degree  $\alpha$  is equal to  $[\text{R}]/2C_0 = I/I_0$ , where  $I$  is the ESR intensity integral, and  $I_0$  is the ESR intensity integral at the asymptotic limit, which is obtained by fitting the curve (Figure 4b). The equilibrium constant  $K$  is related to the dissociation degree  $\alpha$  by eq 1:

$$K = \frac{[\text{R}]^2}{[\text{D}]} = \frac{4\alpha^2}{1 - \alpha} C_0 \quad (1)$$

The bond dissociation enthalpy  $\Delta H^\circ$  can be calculated from van't Hoff's eq 2, where  $\Delta H^\circ$  and  $\Delta S^\circ$  are assumed to be temperature independent in the examined range (40 K):<sup>16</sup>

$$\ln K = -\Delta H^\circ/RT + \Delta S^\circ/R \quad (2)$$

The plot of  $\ln \alpha^2/(1 - \alpha)$  over  $1/T$  (from 270 to 310 K) was fit by linear regression, giving an  $r$  factor of 0.999, from which the bond dissociation enthalpy and entropy were obtained:  $\Delta H^\circ = 11.34 \pm 0.11$  kcal/mol and  $\Delta S^\circ = 14.8 \pm 0.4$  cal  $\text{mol}^{-1}$   $\text{K}^{-1}$  (in  $\text{CCl}_4$ ; Figure 5). The bond dissociation enthalpy of dimer **8a** is thus similar to that of the trityl radical  $\alpha$ ,p-dimer (10.7 kcal/mol).<sup>16a</sup>

The bond dissociation enthalpy of biphenalenyl **8a** in *toluene* in the temperature range of 245–285 K was derived as above, with  $\Delta H^\circ = 9.8 \pm 0.7$  kcal/mol and  $\Delta S^\circ = 11.4 \pm 2.8$  cal  $\text{mol}^{-1}$   $\text{K}^{-1}$ . The slightly smaller enthalpy value ( $\Delta\Delta H^\circ = 1.5$  kcal/mol) in toluene as compared to that in  $\text{CCl}_4$  can be rationalized by the increase in solvation strength through  $\pi$ - $\pi$  interactions of radical **1** with this solvent, which favors the dissociation of dimer **8a**.

The small change ( $\leq 2\%$ ) of radical concentration of the 2-azaphenalenyl radical **2** over the experimentally measurable temperature range (220–330 K) in toluene did not allow quantitative estimation of its dimerization enthalpy (Figure 3).<sup>14</sup> However, it is clear that the stability of radical **2** toward dimerization is significantly increased, with a bond formation enthalpy that is likely small or even slightly positive. This is unusual in that phenalenyl radical derivatives that are stabilized

(15) The absolute radical concentration was obtained by calibration of the ESR intensity integral with a solution of 3-oxo-TEMPO in toluene ( $1.0 \times 10^{-6}$  M): Ohmes, E.; Kothe, G.; Naujok, A.; Zimmermann, H. *Ber. Bunsen-Ges. Phys. Chem.* **1971**, *75*, 895–903.

(16) (a) Neumann, W. P.; Uzick, W.; Zarkadis, A. K. *J. Am. Chem. Soc.* **1986**, *108*, 3762–3770. (b) Lucarini, M.; Pedulli, G.; Cipollone, M. *J. Org. Chem.* **1994**, *59*, 5063–5070.

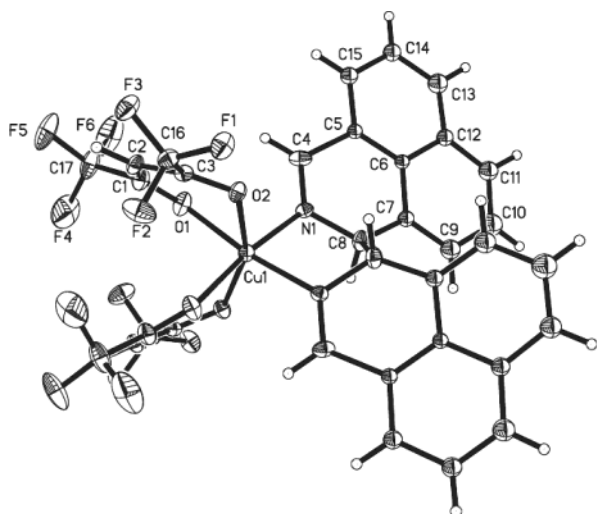


**Figure 6.** X-ray structure of  $\text{Cu}(\text{hfac})_2(1,1'\text{-bi-1H-2-azaphenalene})$  (**11**).

toward  $\sigma$ -dimerization are so because of bulky substituents.<sup>2</sup> It is likely that the lowered SOMO energy of the 2-azaphenaleny radical **2** (Table 2) as compared to that of the phenaleny radical **1** stabilizes it toward dimerization by a few kcal/mol. It is also foreseeable that this stabilization is even larger for the 2,5-diaza- and 2,5,8-triazaphenaleny radicals **3** and **4**, which would be an important asset for use of these parent radicals for metal complexation to form two- and three-dimensional networks.

**Complexation of the 2-Azaphenaleny Radical 2.** Upon attempted complexation of radical **2**, generated in situ by air oxidation of the intermediate 2-azaphenalene **8b**, with  $\text{Cu}(\text{hfac})_2$  (hfac = hexafluoroacetylacetonate), the coordinated complex **11** was formed instead in 50% yield and characterized by X-ray diffraction (Figure 6). Significantly, complex **11** is the first structurally characterized  $\sigma$ -dimer of a phenaleny radical derivative, evidently due to the inherently labile nature of these compounds. The copper(II) center adopts a distorted octahedral coordination geometry with the two ligated nitrogen atoms of the ligand in *cis*-relationship. The C–C single bond connecting the two phenalene units of **2** has a length of 1.583 Å, slightly longer than a normal C–C single bond (1.54 Å). This, on the other hand, is consistent with a weak bond dissociation enthalpy for dimer **12b** even in this complexed state. It is likely that the dimerization of the 2-azaphenaleny radical **2** in this situation is promoted by stabilization of the product through chelate formation,<sup>17</sup> helped in part by the known propensity for the  $\text{Cu}(\text{hfac})_2$  complex to distort to a *cis*-octahedral geometry.<sup>18</sup>

## Conclusion

The 2-azaphenaleny radical **2** has been synthesized and characterized by ESR spectroscopy. Variable-temperature ESR experiments with the phenaleny (**1**) and 2-azaphenaleny (**2**) radicals find that substitution of a CH group by a nitrogen atom appears to stabilize the radical toward dimerization. Attempts to trap radical **2** by complexation with  $\text{Cu}(\text{hfac})_2$  lead to the

$\sigma$ -dimer **12b** chelated with the copper(II) center. Complexation with transition metals having only axial coordination positions available could prevent this dimerization reaction.<sup>17</sup> Further work on the synthesis of a series of parent and substituted 2-aza-, 2,5-diaza-, and 2,5,8-triazaphenaleny radicals, as well as their complexation with transition metal ions, is currently under way.

## Experimental Section

**General Remarks.** All reactions were performed under argon, and ESR spectra were recorded on a Bruker ESP380E spectrometer.

**2,3-Dihydro-(2-phenylmethyl)-1H-benz[de]isoquinoline (5).** Anhydrous aluminum chloride (0.53 g, 4.0 mmol) and  $\text{LiAlH}_4$  (0.15 g, 4.0 mmol) were added to 15 mL of cold, dry THF (ice bath) with stirring. After removal of the ice bath, *N*-benzylphthalimide (0.287 g, 1.0 mmol) was added in small portions. The mixture was stirred at 40 °C for 5.5 h, and then at room temperature for 10 h. The resulting mixture was poured into 100 mL of cold 0.3 N HCl and stirred for 1 h. After filtration, the filtrate was basified with 20% KOH up to pH = 14, and then the amine was extracted with diethyl ether (3 × 100 mL). The organic layer was dried with magnesium sulfate and purified by chromatographic filtration through a pad of silica gel ( $\text{CH}_2\text{Cl}_2/\text{EtOAc}$  4:1) to give compound **5** as a yellow solid (0.23 g, 89%), mp 68–70 °C.  $^1\text{H}$  NMR (500 MHz,  $\text{CDCl}_3$ ):  $\delta$  3.86 (s, 2H), 4.04 (s, 4H), 7.21 (d,  $J = 6.9$  Hz, 2H), 7.35–7.5 (m, 7H), 7.74 (d,  $J = 6.9$  Hz, 2H).  $^{13}\text{C}$  NMR (100 MHz,  $\text{CDCl}_3$ ):  $\delta$  56.4, 61.9, 122.0, 125.6, 126.0, 127.3, 128.2, 128.3, 129.2, 133.1, 133.1, 137.9. IR (KBr): 3030, 2932, 2800, 1600, 1496, 817, 796, 752, 698  $\text{cm}^{-1}$ . HRMS (EI) calcd for  $\text{C}_{19}\text{H}_{16}\text{N}$  ( $[\text{M} - \text{H}]^+$ ), 258.1283; found, 258.1286.

**2,3-Dihydro-1H-benz[de]isoquinoline (6).** To a solution of compound **5** (4.1 g, 16 mmol) in 50 mL of dry dichloromethane was added ethyl chloroformate (2.0 mL, 21 mmol), and the mixture was refluxed for 8 h. The solvent was then removed under reduced pressure, and to the residue was added 120 mL of an ethylene glycol solution of KOH (23 g, 424 mmol) and hydrazine monohydrate (4.0 g, 80 mmol). The mixture was heated under reflux for 4 h, and then poured into water and extracted with diethyl ether. The organic layer was dried with magnesium sulfate. Column chromatography (EtOAc, then MeOH) gave compound **6** as a light yellow solid (2.4 g, 89%), mp 58–60 °C.  $^1\text{H}$  NMR (400 MHz,  $\text{CDCl}_3$ ):  $\delta$  2.23 (br s, 1H), 4.28 (s, 4H), 7.15 (d,  $J = 7.0$  Hz, 2H), 7.40 (dd,  $J_1 = 8.3$ ,  $J_2 = 7.0$  Hz, 2H), 7.71 (d,  $J = 8.3$  Hz, 2H).  $^{13}\text{C}$  NMR (100 MHz,  $\text{CDCl}_3$ ):  $\delta$  49.8, 121.2, 125.6, 126.3, 128.3, 133.5, 134.4. IR (KBr): 3253, 2936, 2847, 1598, 1508, 1052, 910, 820, 794, 772  $\text{cm}^{-1}$ . HRMS (EI) calcd for  $\text{C}_{12}\text{H}_{10}\text{N}$  ( $[\text{M} - \text{H}]^+$ ), 168.0813; found, 168.0808.

***N*-Chloro-2,3-dihydro-1H-benz[de]isoquinoline (7).** To a solution of compound **6** (50 mg, 0.3 mmol) in 20 mL of diethyl ether was added a suspension of *N*-chlorosuccinimide (39 mg, 0.3 mmol) in 10 mL of diethyl ether at 0 °C. The mixture was stirred for 30 min at 0 °C. After filtration, the filtrate was concentrated and passed through a pad of silica gel ( $\text{CH}_2\text{Cl}_2$ ) to give compound **7** as a light yellow solid (60 mg, 98%), mp > 30 °C (dec).  $^1\text{H}$  NMR (500 MHz,  $\text{CDCl}_3$ ):  $\delta$  4.65 (s, 4H), 7.22 (d,  $J = 7.1$  Hz, 2H), 7.45 (dd,  $J_1 = 8.3$ ,  $J_2 = 7.0$  Hz, 2H), 7.77 (d,  $J = 8.3$  Hz, 2H).  $^{13}\text{C}$  NMR (125 MHz,  $\text{CDCl}_3$ ):  $\delta$  64.2, 122.6, 125.8, 126.8, 126.9, 131.0, 132.8. IR (KBr): 2950, 1600, 1507, 1395, 1368, 1337, 1262, 821, 798, 772, 722, 577  $\text{cm}^{-1}$ . HRMS (EI) calcd for  $\text{C}_{12}\text{H}_{10}\text{NCl}$  ( $\text{M}^+$ ), 203.0502; found, 203.0508.

### Generation of 3H-Benz[de]isoquinoline **8b** for Characterization.

To a solution of compound **7** (5 mg, 0.025 mmol) in 1 mL of  $\text{CD}_2\text{Cl}_2$  in a standard NMR tube was added triethylamine (0.05 mL, 0.36 mmol). After the solution was left standing for 25 min, the  $^1\text{H}$  NMR spectrum was recorded, and then immediately thereafter the mass spectrum of **8b** was taken (UCLA Mass Spectrometry facility).  $^1\text{H}$  NMR (500 MHz,  $\text{CD}_2\text{Cl}_2$ ):  $\delta$  5.44 (br d,  $J = 2.7$  Hz, 2H), 7.29 (m, 2H), 7.45 (m, 2H), 7.64 (d,  $J = 8.2$  Hz, 1H), 7.79 (d,  $J = 8.7$  Hz, 1H), 8.48 (t,  $J = 2.7$  Hz, 1H). HRMS (EI) calcd for  $\text{C}_{12}\text{H}_9\text{N}$  ( $\text{M}^+$ ), 167.0735; found,

(17) In an attempt to block the  $\sigma$ -dimerization of radical **2**, complexation was performed with the dinuclear complex  $\text{Rh}_2(\text{CF}_3\text{COO})_4$ , which has only axial coordination positions available. A green powder of a new complex precipitated, which is ESR active. However, because radical **2** cannot be obtained in pure form due to its reactivity with excess air (as found through attempts at crystallization) or with silica gel upon attempted chromatography, full characterization could not be performed. The solid likely is a mixture of 1:1 and 1:2 rhodium complexes with radical **2** (IR).

(18) Pradilla-Sorzano, J.; Fackler, J. P., Jr. *Inorg. Chem.* **1973**, *12*, 1174–1182.

167.0731. The sample also has significant but varying amounts of oxidation byproduct ( $C_{12}H_7NO$ ) even under the most careful handling.

**Preparation of the 2-Azaphenalenyl Radical 2 Solution and ESR Determination of Spin Concentration.** To a solution of compound **7** (1 mg, 0.005 mmol) in 1 mL of  $CH_2Cl_2$  was added triethylamine (0.05 mL, 0.5 mmol). The resulting solution was stirred for 1 h, and the color of the solution turned to blue (this color may be due to traces of the anion); then the solvent was evaporated in vacuo. The resulting yellow green solid was redissolved in toluene (0.5 mL). After filtration to remove the triethylamine hydrochloride, the toluene solution was transferred in a standard ESR quartz tube under air and sealed. After the solution was left standing for 2 days, the ESR spectrum of **2** was recorded. Variable-temperature ESR experiments were performed on this sample after standing for 2 months to allow all of the oxygen to react. Absolute radical concentrations were determined by calibration with a toluene solution of the 3-oxo-TEMPO radical as a reference.<sup>15</sup>

**Preparation of a Solution of the Phenalenyl Radical 1.** Phenalene (1.0 mg), prepared according to the literature procedure,<sup>19</sup> was dissolved in 0.5 mL of toluene or  $CCl_4$  and sealed in a quartz tube under air. Variable-temperature ESR studies were performed after letting the solution stand for 2 months or by "aging" the sample in  $CCl_4$  as described in the text. Absolute radical concentrations were determined from the ESR signal intensities calibrated to a toluene solution of the 3-oxo-TEMPO radical of known concentration.<sup>15a</sup>

**(1,1'-Bi-1*H*-2-azaphenalene) Bis(hexafluoroacetylacetonato)-copper(II) Complex 11.** To a solution of compound **7** (20 mg, 0.1 mmol) and copper(II) hexafluoroacetylacetonate (50 mg, 0.1 mmol) in

5 mL of toluene was added *N,N*-diisopropylethylamine (0.051 mL, 0.3 mmol) under argon. The mixture was stirred for 24 h at room temperature. After filtration, the filtrate was layered with hexane under argon but with no special precaution to avoid exposure to some air. The mixture was allowed to stand at  $-20\text{ }^\circ\text{C}$  for 1 week. Dark green single crystals (30 mg, 50%, based on  $Cu(hfac)_2$ ) were obtained for X-ray crystallography. IR (KBr): 1708, 1681, 1256, 1148, 670  $cm^{-1}$ . MS (FAB<sup>+</sup>) calcd for  $C_{29}H_{17}F_6N_2O_2Cu$ , 602.1; found, 602.3.

**Crystal Structure Determination.** Copper(II) complex **11** crystallized in the monoclinic space group  $C2/c$ , with  $a = 21.593(3)\text{ \AA}$ ,  $b = 14.056(3)\text{ \AA}$ ,  $c = 16.127(3)\text{ \AA}$ ,  $\beta = 130.540(5)^\circ$ ,  $Z = 4$ ,  $V = 3719.7(12)\text{ \AA}^3$ . Data were collected at 100 K on a Bruker Smart 1000 CCD diffractometer using graphite-monochromated Mo  $K\alpha$  radiation, to a maximum  $2\theta = 56.66^\circ$ , giving 11 827 reflections collected, 4438 unique ( $R_{int} = 0.07461$ ). The structure was solved by direct methods and refined with full matrix least squares, yielding  $R = 0.0611$ ,  $wR = 0.1230$ , and  $GOF = 0.888$  with a cutoff  $I > 2\sigma I$ .

**Acknowledgment.** We are thankful to Miguel Garcia-Garibay and Karoly Holczer at UCLA for helpful discussions on the ESR experiments, the NSF for grants CHE-0080942 (Y.R.), CHE-9871332 (X-ray), CHE-9974928 (NMR), the Alfred P. Sloan Research Foundation, and NIH-S10RR15952 (MS).

**Supporting Information Available:** Crystallographic data for complex **11**. This material is available free of charge via the Internet at <http://pubs.acs.org>.

(19) (a) Lewis, I. K.; Topsom, R. D. *Aust. J. Chem.* **1965**, *18*, 923–925. (b) Pagni, R. M.; Watson, C. R. *Tetrahedron* **1973**, *29*, 3807–3810.

JA029236O